ECS Journal of Solid State Science and Technology, **1** (1) R54-R56 (2012)
2162-8769/2012/1(1)/R54/3/$28.00 © The Electrochemical Society

Semipolar GaN Films on Prism Stripe Patterned *a*-Plane Sapphire Substrates

Cheng-Yu Hsieh, Bo-Wen Lin, Wen-Hao Cheng, Bau-Ming Wang, Li Chang,[z] and YewChung Sermon Wu[*,z]

Department of Materials Science and Engineering, National Chiao Tung University, Hsinchu 300, Taiwan

A $(1\,0\,\bar{1}\,4)$ semipolar GaN layer was grown on periodic stripe patterned *a*-plane sapphire substrate fabricated by using two-steps etching process. The stripes in prism shape were inclined with sapphire *c*-axis in 60 degrees. The orientation relationship between semipolar GaN and sapphire is $(0\,0\,0\,2)_{GaN}//(2\,\bar{1}\,\bar{1}\,\bar{3})_{sapphire}$ and $[2\,\bar{1}\,\bar{1}\,0]_{GaN}//[2\,3\,\bar{5}\,2]_{sapphire}$ as defined by selected area diffraction in transmission electron microscopy (TEM). Growth of semipolar GaN on the sidewalls of the prism stripes is evidenced from TEM and X-ray φ scan. The quality of semipolar GaN film is reasonably good as examined with X-ray rocking curves. In addition, TEM and cathodoluminescence results show that the dislocation density in the semipolar GaN is significantly reduced near the film surface.
© 2012 The Electrochemical Society. [DOI: 10.1149/2.006201jss] All rights reserved.

Manuscript submitted January 11, 2012; revised manuscript received March 20, 2012. Published July 17, 2012.

GaN-based light-emitting diodes (LED) have been used for solid state lighting. SiC and sapphire are commonly used as substrate for *c*-plane GaN growth. Recently, various forms of patterned sapphire substrates are widely used to obtain high brightness GaN-based LEDs.[1–3] Although the quality of GaN films has been improved, it still suffers the strong spontaneous polarization along *c*-axis which reduces the light emitting efficiency, known as quantum confined stark effect (QCSE), and the internal electric field can also cause redshift of the emitting light wavelength from muti-quantum well.[4–6] In view of this, nonpolar and semipolar GaN films are expected to eliminate or reduce the QCSE effect. However, it is difficult to grow high quality non-polar and semipolar GaN crystals. For growth of nonpolar *a*-plane GaN on sapphire substrate, *r*-plane sapphire is commonly used. Nevertheless, it always accompanies with a high density of threading dislocations and a high density of stacking faults in GaN film as a result of large lattice misfit.[7,8] If a hemispherical pattern was applied on the *r*-plane sapphire, it was able to reduce the defect density.[9–11] Okada and Okuno have reported that nonpolar *m*-plane GaN films can be grown on patterned *a*-plane sapphire substrates if a pattern with *c*-plane sidewalls is adopted.[12–14]

In this study, periodic prism stripe patterns were introduced onto *a*-plane sapphire substrates for GaN growth. As a result, semipolar GaN can be obtained as shown by the evidence of microstructural characterization using X-ray diffraction, transmission electron microscopy, and cathodoluminescence mapping.

Experimental

Patterned *a*-plane sapphire substrates with a periodic stripe array were employed to grow GaN. 2-inch patterned sapphire substrate (PSS) was first prepared by standard photolithography using photoresist pattern as the dry-etching mask of 300 nm SiO_2. The pattern was in the prism-shaped stripes with a period of 4.0 μm (openings: 2.0 μm) and the height of prisms was 0.8 μm. The pattern was first defined by inductively coupled plasma (ICP) with BCl_3 as etchant,[15–21] followed by etching in hot H_3PO_4–based solution (at a temperature ranged from 270 to 300°C).[22,23] The stripe direction was about *m*-direction +30° toward *c*-direction (i.e., inclined with sapphire *c*-axis in 60°) as shown in Fig. 1a. Scanning electron microscopy (SEM) observation in Fig. 1b shows the surface morphology of the prism array pattern on PSS.

After cleaning, GaN films were grown by metal-organic chemical vapor deposition (MOCVD). An AlN buffer layer (30 nm) was firstly grown at 850°C on PSS, followed by growth of GaN (>7 μm) at 1100°C with III/V ratio of about 1500. Trimethylgallium (TMG), trimethylaluminum (TMA) and ammonia (NH_3) were used as gallium, aluminum and nitrogen sources, respectively. Hydrogen (H_2) was used as the carrier gas for TMG and TMA. For comparison, GaN on an unpatterned *a*-plane sapphire substrate was also grown with the same MOCVD condition.

High-resolution X-ray diffraction (HRXRD), SEM, and transmission electron microscopy (TEM) with selected area diffraction were used to characterize crystalline quality, surface morphology, microstructure, and orientation relationship. HRXRD was performed in a Bruker D8 diffractometer (wavelength of Cu $K_{\alpha 1}$ 1.54051 Å). SEM and TEM examinations were carried out in a JEOL 7000 SEM microscope and a JEOL 2100F TEM microscope. Cross-sectional SEM and TEM specimens were prepared by focused ion beam (FIB, FEI nanolab NOVA 200) with 30 kV Ga^+ ion beam. Also, the defect distribution was examined with cathodoluminescence (CL) maps (JEOL 7001F SEM).

Results and Discussion

Figure 1c shows a plan-view SEM image of the GaN layer grown on PSS, revealing that the surface consists of periodic grooves and symmetrically inclined plates. From the cross-sectional SEM image in Fig. 1d, two characteristic V-shape features of surface grooves on the GaN film can be periodically observed. On top of each prism a shallow groove (1 μm depth) of GaN is aligned with the ridgeline of

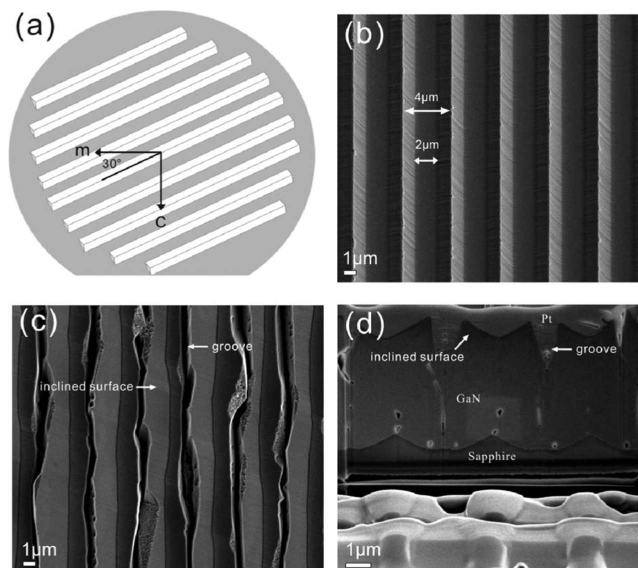

Figure 1. (a) Schematic pattern diagram of PSS with crystallographic directions. SEM images showing (b) prism line pattern, (c) plan-view of GaN film surface, and (d) cross-section of GaN on PSS.

*Electrochemical Society Active Member.
zE-mail: lichang@cc.nctu.edu.tw; SermonWu@stanfordalumni.org

Downloaded on 2014-04-28 to IP 140.113.38.11 address. Redistribution subject to ECS terms of use (see ecsdl.org/site/terms_use) unless CC License in place (see abstract).

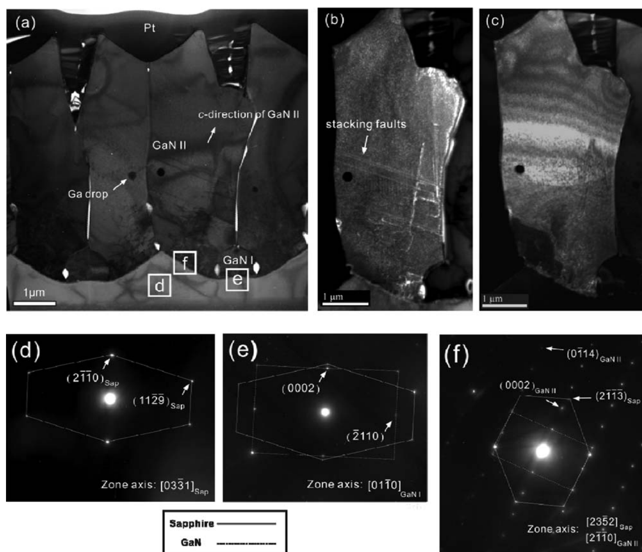

Figure 2. Cross-sectional TEM image of GaN on PSS (a) bright-field, and (b) and (c) dark-field images ($\mathbf{g} = 0002$ and $01\bar{1}0$ tilt from zone axis $[2\bar{1}\bar{1}0]_{\mathrm{GaN\ II}}$). Selected area diffraction patterns of (d) sapphire in zone axis, (e) GaN I in $[01\bar{1}0]$ zone axis with sapphire in $[\bar{3}301]$, and (f) GaN II $[2\bar{1}\bar{1}0]$ zone axis and sapphire in $[23\bar{5}2]$. The black dots in (a) are Ga drops formed from FIB ion milling.

the prism pattern and the inclined angle of facets on the GaN film is about 34° inclination with sapphire a-plane. Between adjacent GaN grains above the bottom region of the pattern, a deep surface groove was formed as well. It can also be found that a number of voids appear around ridgelines and bases of the patterns.

To characterize the microstructure of GaN on PSS, TEM specimens were specifically prepared with the cross section perpendicular to PSS stripe lines. The bright-field (BF) and dark-field (DF) TEM images with selected area diffraction patterns (SADPs) are shown in Fig. 2. As shown in Figs. 2a, the main characteristic features are similar to those seen in SEM. The prism in the PSS has a height of 0.8 μm and the sidewall length of 1.63 μm with 31° to the sapphire surface which has a flat base of 2 μm. Two kinds of GaN grains at different locations are observed with dissimilar morphology: one in a height of 1 μm is just above the base bottom region (GaN I) and the other is in contact with the sidewalls of the prism on the sapphire pattern (GaN II) and extend ~7 μm to the top surface of the GaN film. It is noticed that the GaN I is completely enclosed by GaN II type grains.

The DF images in Figs. 2b and 2c were taken under different diffraction vectors from zone axis $[2\bar{1}\bar{1}0]$ of GaN II. It can be clearly seen in Figs. 2a and 2b that parallel stacking faults exist in GaN II and they are 28.8° deviated from sapphire *a*-plane. In Figs. 2a and 2c almost no dislocations can be observed in the upper half region of GaN II. As shown in magnified TEM images in Fig. 3 around the interface between GaN II and the sidewall of PSS, quite a number of threading dislocations are seen to be almost deviated from the growth direction of GaN II along *c*-axis, and most of them bend to the boundaries between GaN grains after growth of about 2 μm. As a result, the upper half area of GaN is almost dislocation free. The SADP in Fig. 2d is the zone axis pattern of sapphire along $[03\bar{3}1]_{\mathrm{sapphire}}$, indicating that the stripe direction in PSS is parallel to $[03\bar{3}1]_{\mathrm{sapphire}}$ which is m+c direction in agreement with the angle measured by plan-view SEM. From the SEM and TEM images, the angle between the sidewall and sapphire substrate surface (*a*-plane) is measured to be 31° from which the plane of the sidewall can be determined to be $(4\bar{1}\bar{3}\bar{6})$ from the crystallography based on the zone axis SADP.

Figure 2e is a SADP from region e in Fig. 2a which shows GaN I $[01\bar{1}0]_{\mathrm{GaN\ I}}$ zone axis pattern with sapphire $[03\bar{3}1]_{\mathrm{sapphire}}$ one. Therefore, the orientation relationship between GaN I and sapphire can be established as $(0001)_{\mathrm{GaN}}//(11\bar{2}0)_{\mathrm{sapphire}}$ and $[01\bar{1}0]_{\mathrm{GaN}}//[03\bar{3}1]_{\mathrm{sapphire}}$ which is different from the orientation relationship of $(0001)_{\mathrm{GaN}}//(11\bar{2}0)_{\mathrm{sapphire}}$ and $[01\bar{1}0]_{\mathrm{GaN}}//[0001]_{\mathrm{sapphire}}$ usually observed for MOCVD grown GaN on unpatterned blanket *a*-plane sapphire.[24] GaN II grains grown from both inclined sidewalls of a prism are contacted with each other above the ridge, whereas GaN II grains from the opposite faces of adjacent prisms are in contact above the middle of the pattern base. As the GaN II grains were grown in opposite directions, they formed the groove region on film surface. The orientation relationship between GaN II and sapphire is determined from SADP in Fig. 2f obtained from region f which covers both the GaN II and the sapphire sidewall of the prism. The SADP is in zone axis of $[23\bar{5}2]_{\mathrm{sapphire}}$ which is about 21.4° tilted away from $[03\bar{3}1]_{\mathrm{sapphire}}$ by ~11° in-plane rotation along a-plane sapphire and inclined tilt of ~18° away from the plane. It is seen that the GaN in the SADP can be indexed as $[2\bar{1}\bar{1}0]$ zone axis pattern and the orientation relationship is derived as $(0002)_{\mathrm{GaN\ II}}//(2\bar{1}\bar{1}\bar{3})_{\mathrm{sapphire}}$ and $[2\bar{1}\bar{1}0]_{\mathrm{GaN\ II}}//[23\bar{5}2]_{\mathrm{sapphire}}$. On a periodic dot prism pattern fabricated on *a*-plane PSS, similar crystallographic relationship of GaN on the sidewall of a dot prism with sapphire has also been shown in our previous study.[25] Interestingly, it has been demonstrated that *c*-plane GaN overgrows over inclined GaN on dot PSS, opposite to the present case that they are overgrown by the inclined GaNs on stripe PSS. The difference between these two cases is under investigation.

From the above analyzes, it is shown that the GaN II grain is grown along the *c*-axis of GaN which is normal to $(2\bar{1}\bar{1}\bar{3})_{\mathrm{sapphire}}$ and tilts about 28.8° from the substrate normal. From SADPs (not shown), it can be proved that GaN II grains grown on the opposite sides of the prism exhibit the same orientation relationship with sapphire. Further confirmation is obtained from XRD φ scan of GaN II (0002) and sapphire $(2\bar{1}\bar{1}\bar{3})$ as shown in Fig. 4. From the orientation relationship, one can deduce that GaN $(01\bar{1}4)$ is about 7° deviated from the

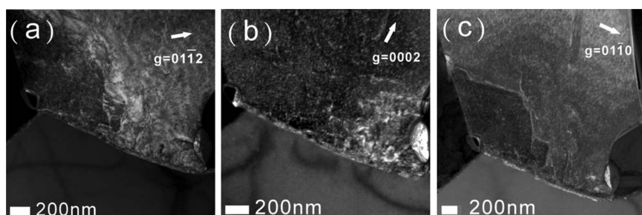

Figure 3. Magnified DF TEM images of GaN on PSS near sidewall under (a) with $\mathbf{g} = 01\bar{1}2$, (b) with $\mathbf{g} = 0002$, and (c) with $\mathbf{g} = 01\bar{1}0$, tilt from zone axis $[2\bar{1}\bar{1}0]_{\mathrm{GaN\ II}}$.

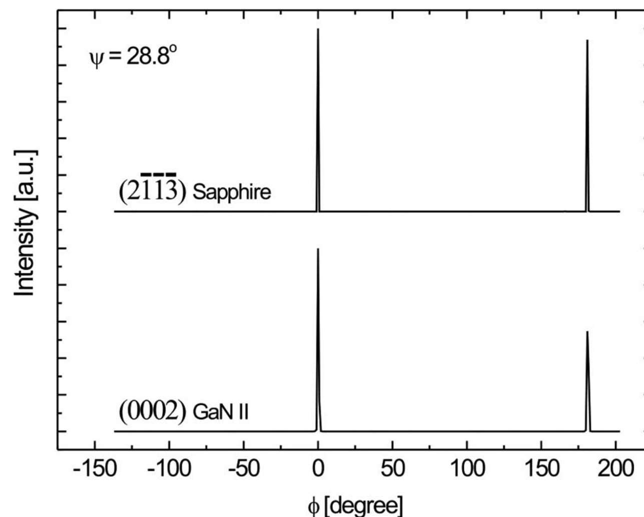

Figure 4. X-ray off-axis φ-scans for sapphire $(2\bar{1}\bar{1}\bar{3})$ and GaN (0002) reflections. The angle of inclination used to access the off-axis reflection for each scan is also included.

Downloaded on 2014-04-28 to IP 140.113.38.11 address. Redistribution subject to ECS terms of use (see ecsdl.org/site/terms_use) unless CC License in place (see abstract).

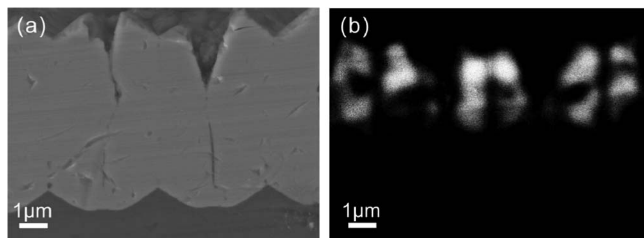

Figure 5. (a) Cross-sectional SEM image of GaN film and (b) the corresponding monochromated (370 nm) CL map of GaN film. The bright regions in CL map correspond to top region of GaN film in SEM image.

sapphire *a*-plane and is found to be the plane nearly parallel to *a*-plane sapphire substrate surface. Therefore, the GaN layer grown on the *a*-plane PSS is a semipolar one.

The GaN quality is also examined with X-ray rocking curves (XRCs) and CL maps. For GaN II, the full width at half maximum (fwhm) values of $(0\,0\,0\,2)$ and $(0\,1\,\bar{1}\,4)$ XRCs are 910 and 868 arcsec, respectively, suggesting that the GaN II may have a reasonably good quality. Figures 5a and 5b are a SEM image and a corresponding monochromated CL map taken at wavelength of 370 nm, respectively. Clearly, the upper region of the GaN film exhibits bright contrast in the CL map of Fig. 5b which corresponds to strong excitation with a very low density of non-radiation centers in this region except around boundaries. In contrast, the lower region appears dark contrast, implying that it is highly defected. This result agrees with TEM observations in that most of dislocations and stacking faults are observed in the bottom half region of GaN II, whereas the upper half is nearly defect free. The improvement of film quality with thickness is likely due to bending of threading dislocations in the bottom half region without further extending to the upper region during growth. However, the reason for bending is not clear yet at the moment which needs further investigation.

Conclusions

In summary, a $(0\,1\,\bar{1}\,4)$ semipolar GaN layer has been grown on a prism stripe patterned *a*-plane sapphire substrate. The pattern was fabricated by two step etching process and the stripe line of pattern is aligned to $[0\,3\,\bar{3}\,1\,]_{sapphire}$. The sidewalls of prisms are identified as $(4\,\bar{1}\,\bar{3}\,\bar{6}\,)_{sapphire}$ by TEM. On the sidewalls, GaNs are grown with their *c*-plane//$(2\,\bar{1}\,\bar{1}\,\bar{3})_{sapphire}$, such that semipolar GaN is formed with $(0\,1\,\bar{1}\,4)$ orientation in about 7° deviated from a-plane sapphire surface. TEM results and CL maps show that the semipolar GaN film has a low defect density after growth to 2 μm thickness. The threading dislocations from the sidewalls are found to extend along *c*-axis of GaN and laterally bend to GaN boundaries, resulting in a defect-free region with further growth.

Acknowledgments

This project was funded by Sino American Silicon Products Incorporation and the National Science Council of Republic of China under grant No. 98-2221-E009-041-MY3. Technical supports from National Nano Device Laboratory, Center for Nano Science and Technology, Nano Facility Center and Semiconductor Laser Technology Laboratory of National Chiao Tung University are also acknowledged. The authors thank H.C. Kuo for valuable discussions.

References

1. J. H. Cheng, Y. C. S. Wu, W. C. Liao, and B. W. Lin, *Appl. Phys. Lett.*, **96**, 051109 (2010).
2. Y. S. Lin, K. H. Lin, Y. M. Chang, and J. A. Yeh, *Surf. Sci.*, **606**, L1–L4(2012).
3. N. Okada, H. Oshita, K. Yamane, and K. Tadatomo, *Appl. Phys. Lett.*, **99**, 242103 (2011).
4. D. A. B. Miller, D. S. Chemla, T. C. Damen, A. C. Gossard, W. Wiegmann, T. H. Wood, and C. A. Burrus, *Phys. Rev. Lett.*, **53**, 2173 (1984).
5. K. Tanaka, N. Kotera, and H. Nakamura, *IEEE Elec. Lett.*, **34**, 2163 (1998).
6. T. Takeuchi, S. Sota, M. Katsuragawa, M. Komori, H. Takeuchi, H. Amano, and I. Akasaki, *Jpn. J. Appl. Phys.*, **36**, L382 (1997).
7. J. Smalc-Koziorowska, G. Tsiakatouras, A. Lotsari, A. Georgakilas, and G. P. Dimitrakopulos, *J. Appl. Phys.*, **107**, 073525 (2010).
8. R. Hao, M. J. Kappers, M. A. Moram, and C. J. Humphreys, *J. Cryst. Growth*, **337**, 81 (2011).
9. Z. H. Wu, Y. Q. Sun, J. Yin, Y.-Y Fang, J. N. Dai, C. Q. Chen, Q. Y. Wei, T. Li, K. W. Sun, A. M. Fischer, and F. A. Ponce, *J. Vac. Sci. Technol. B*, **29**, 2 (2011).
10. Y. Q. Sun, Z. H. Wu, J. Yin, Y. Y. Fang, H. Wang, C. H. Yu, X. Hui, C. Q. Chen, Q. Y. Wei, T. Li, K. W. Sun, and F. A. Ponce, *Thin Solid Films*, **519**, 2508 (2011).
11. G. H. Yoo, H. S. Park, H. J. Lim, S. G. Lee, O. Y. Nam, Y. B. Moon, C. Lim, B. Y. Kong, H. K. Cho, and H. K. J *pn. J. Appl. Phys.*, **50**, 042103 (2011).
12. N. Okada, Y. Kawashima, and K. Tadatomo, *Appl. Phys. Exp.*, **1**, 111101 (2008).
13. K. Okuno, Y. Saito, S. Boyama, N. Nakada, S. Nitta, R. G. Tohmon, Y. Ushida, and N. Shibata, *Appl. Phys. Exp.*, **2**, 031002 (2009).
14. N. Okada, Y. Kawashima, and K. Tadatomo, *Phys. Status Solidi A*, **206**, 6 (2009).
15. D. S. Wuu, W. K. Wang, W. C. Shih, R. H. Horng, C. E. Lee, W. Y. Lin, and J. S. Fang, *IEEE Photon. Tech. Lett.*, **17**, 288 (2005).
16. Z. H. Feng and K. M. Lau, *IEEE Photon. Technol. Lett.*, **17**, 1812 (2005).
17. W. Wang, D. Wuu, W. Shih, J. Fang, C. Lee, W. Lin, P. Han, R. Horng, T. Hsu, T. Huo, M. Jou, A. Lin, and Y. Yu, *Jpn. J. Appl. Phys.*, **44**, 2512 (2005).
18. C. F. Shen, S. J. Chang, W. S. Chen, T. K. Ko, C. T. Kuo, and S. C. Shei, *IEEE Photon. Tech. Lett.*, **19**, 780 (2007).
19. D. Kang, J. Song, B. Shim, E. Ko, D. Kim, S. Kannappan, and C. Lee, *Jpn. J. Appl. Phys.*, **46**, 2563 (2007).
20. R. H. Horng, W. K. Wang, S. C. Huang, S. Y. Huang, S. H. Lin, C. F. Lin, and D. S. Wuu, *J. Cryst. Growth*, **298**, 219 (2007).
21. J. Lee, J. Oh, S. Choi, Y. Kim, H. K. Cho, and J. Lee, *IEEE Photon. Tech. Lett.*, **20**, 345 (2008).
22. F. Dwikusuma, D. Saulys, and T. F. Kuech, *J. Electrochem. Soc.*, **149**, G603 (2002).
23. H. Gao, F. Yan, Y. Zhang, J. Li, Y. Zeng, and G. Wang, *J. Appl. Phys.*, **103**, 014314 (2008).
24. T. Paskova, V. Darakchieva, E. Valcheva, P. P. Paskov, B. Monemar, and M. Heuken, *Phys. Status Solidi B*, **240**, 318 (2003).
25. B. W. Lin, C. C. Chang, C. Y. Hsieh, B. M. Wang, Y. C. S. Wu, and W. C. Hsu, *IEEE Photon. Tech. Lett.*, **23**, 1772 (2011).

Downloaded on 2014-04-28 to IP 140.113.38.11 address. Redistribution subject to ECS terms of use (see ecsdl.org/site/terms_use) unless CC License in place (see abstract).